ON THE CONTACT OZSVÁTH-SZABÓ INVARIANT

TOLGA ETGÜ AND BURAK OZBAGCI

ABSTRACT. Sarkar and Wang proved that the hat version of Heegaard Floer homology group of a closed oriented 3-manifold is combinatorial starting from an arbitrary nice Heegaard diagram and in fact every closed oriented 3-manifold admits such a Heegaard diagram. Plamenevskaya showed that the contact Ozsváth-Szabó invariant is combinatorial once we are given an open book decomposition compatible with a contact structure. The idea is to combine the algorithm of Sarkar and Wang with the recent description of the contact Ozsváth-Szabó invariant due to Honda, Kazez and Matić. Here we observe that the hat version of the Heegaard Floer homology group and the contact Ozsváth-Szabó invariant in this group can be combinatorially calculated starting from a contact surgery diagram. We give detailed examples pointing out to some shortcuts in the computations.

0. INTRODUCTION

We know that every closed contact 3-manifold (Y,ξ) can be obtained by a contact ± 1 surgery on a Legendrian link in the standard contact S^3 ([3]). It is often convenient to describe (Y,ξ) by a surgery diagram on the plane, i.e., by the projection of a Legendrian link in the standard contact $(\mathbb{R}^3, ker(dz+xdy))$ onto the yz-plane with a ± 1 surgery coefficient assigned to each component of the link. Let s_ξ denote the $Spin^c$ structure induced by ξ. In order to calculate the Heegaard Floer homology group $\widehat{HF}(-Y,s_\xi)$ and in particular to identify the contact Ozsváth-Szabó invariant $c(\xi)\in\widehat{HF}(-Y,s_\xi)$ we first find a suitable open book decomposition compatible with (Y,ξ) using the algorithm in [1] (see also [8],[17],[14],[18],[6],[7],[2]) and then construct a compatible Heegaard diagram for $-Y$ as in [9] which also includes a description of a certain cycle descending to $c(\xi)$ in $\widehat{HF}(-Y,s_\xi)$. Next we convert this Heegaard diagram into a nice Heegaard diagram ([16]) applying some finger moves without affecting the homology class $c(\xi)$ — no handle slides are necessary [15]. Finally we calculate $\widehat{HF}(-Y,s_\xi)$ and $c(\xi)\in\widehat{HF}(-Y,s_\xi)$ by simply counting certain squares and bigons in this nice Heegaard diagram. In fact this procedure will allow us to calculate $\widehat{HF}(-Y)\cong\widehat{HF}(Y)$, not just $\widehat{HF}(-Y,s_\xi)$.

2000 *Mathematics Subject Classification.* 57R17, 57R65, 57R58, 57M99.

Key words and phrases. Heegaard Floer homology, Ozsváth-Szabó invariants, contact structures, open book decomposition .

We note that each step of the suggested combination of the above algorithms can be quite involved and one would like to reduce the calculations as much as possible by making certain choices. Here we demonstrate the significance of a particular choice in simplifying the calculations.

We assume that the reader is familiar with the basics of the Heegaard Floer theory (see [12], [13]). We will work with $\mathbb{Z}_2$ coefficients in our calculations throughout this paper.

1. The contact Ozsváth-Szabó invariant is combinatorial

Theorem 1. *Let (Y,ξ) be a closed contact 3-manifold described by a contact surgery diagram on the plane. We observe that the $Spin^c$ structure s_ξ, Heegaard Floer homology groups $\widehat{HF}(-Y,s_\xi) \subseteq \widehat{HF}(Y)$ and the contact Ozsváth-Szabó invariant $c(\xi) \in \widehat{HF}(-Y,s_\xi)$ can be calculated combinatorially.*

Proof. Let (Y,ξ) be a closed contact 3-manifold described by a contact surgery diagram on the plane, i.e., by the projection of a Legendrian link in the standard contact

$$(\mathbb{R}^3, ker(dz+xdy)) \subset (S^3,\xi_{st})$$

onto the yz-plane with a ± 1 surgery coefficient assigned to each component of the link. First we use the algorithm in [1] (see also [8],[17],[14],[18],[6],[7],[2]) to find an explicit open book decomposition compatible with (Y,ξ). The idea in [1] is to embed the Legendrian surgery link into the pages of an open book decomposition in S^3 compatible with its standard contact structure and then perform the required contact surgeries to obtain an open book decomposition OB_ξ of Y compatible with the resulting contact structure ξ.

Next we briefly recall ([9]) how to get a Heegaard diagram for $-Y$ which also includes a cycle that descends to the contact Ozsváth-Szabó invariant $c(\xi)$ starting from a given open book decomposition OB_ξ of Y compatible with ξ. The open book decomposition OB_ξ can be described as follows: Let S denote the page and let $h : S \to S$ denote the monodromy of OB_ξ. Then Y is homeomorphic to $S\times[0,1]/\sim$, where the equivalence relation is given by

$$(p,1) \sim (h(p),0), \quad p \in S$$

$$(p,t) \sim (p,t'), \quad p \in \partial S;\ t,t' \in [0,1].$$

It is not too hard to see that $Y = H_1 \cup H_2$ is a Heegaard splitting of Y, where $H_1 = S\times[0,1/2]/\sim$ and $H_2 = S\times[1/2,1]/\sim$. Let S_0 and $S_{1/2}$ denote $S\times\{0\}$ and $S\times\{1/2\}$ in H_1, respectively. A basis on a compact surface S with boundary is just a collection of properly embedded disjoint arcs $\{a_1,\dots,a_n\}$ on S such that when we cut S along these arcs we get a single polygon. Now we choose a basis $\{a_1,\dots,a_n\}$ on the page S and choose a point z in the polygonal region mentioned above. Consider the closed surface $\Sigma = S_{1/2} \cup -S_0$ and glue the arc a_i on $S_{1/2}$ with the arc a_i on $-S_0$ to obtain a closed curve

α_i on Σ. Let b_i be an arc which is isotopic to a_i by a small isotopy so that the following hold:

(1) The endpoints of a_i are isotoped along $\partial S_{1/2}$, in the direction given by the orientation of $S_{1/2}$.

(2) The arcs a_i and b_i intersect transversely in one point x_i in the interior of $S_{1/2}$.

(3) If we orient a_i, and b_i is given the induced orientation from the isotopy, then the sign of the intersection of a_i and b_i at x_i is $+1$.

Then consider the arc $h(b_i)$ on $-S_0$ and glue the arc b_i and $h(b_i)$ to get a closed curve β_i on Σ. If we let $\alpha = \{\alpha_1, \ldots, \alpha_n\}$ and $\beta = \{\beta_1, \ldots, \beta_n\}$, then $(\Sigma, \beta, \alpha, z)$ is a Heegaard diagram for $-Y$, while $(\Sigma, \alpha, \beta, z)$ is a Heegaard diagram for Y. Moreover $X = \{x_1, \ldots, x_n\} \in \mathbb{T}_\alpha \cap \mathbb{T}_\beta \subset Sym^n(\Sigma)$ is a cycle in $\widehat{CF}(\Sigma, \beta, \alpha, z)$ which descends to the contact Ozsváth-Szabó invariant $c(\xi) \in \widehat{HF}(-Y)$, where $\mathbb{T}_\alpha = \alpha_1 \times \cdots \times \alpha_n$ and $\mathbb{T}_\beta = \beta_1 \times \cdots \times \beta_n$. Furthermore there is a map from the set of generators $\mathbb{T}_\alpha \cap \mathbb{T}_\beta$ of $\widehat{CF}(\Sigma, \beta, \alpha, z)$ to the set of $Spin^c$ structures on Y. It turns out ([13]) that the special cycle X corresponds to the $Spin^c$ structure s_ξ induced by ξ. Therefore $c(\xi)$ belongs to $\widehat{HF}(-Y, s_\xi) \subseteq \widehat{HF}(-Y)$. We note that $c_1(\xi) = c_1(s_\xi) \in H^2(Y; \mathbb{Z})$ can be calculated ([4]) combinatorially from a given contact surgery diagram of ξ (see page 195 in [11]).

A connected component of the complement of α and β curves in Σ is called a region. Now we use the algorithm of [16] to convert this Heegaard diagram into a nice Heegaard diagram, which we still denote by $(\Sigma, \beta, \alpha, z)$, so that all the regions on Σ not including the base point z are bigons and squares. In general we would need to apply finger moves and handle slides of the β curves in the Heegaard diagram. Handle slides, fortunately, do not arise in our case [15] and a finger move corresponds to a certain kind of isotopy of the β curves.

Recall that a domain is a formal linear combination of the regions on Σ. A domain D is called an empty embedded $2m$-gon from A to B, where $A, B \in \mathbb{T}_\alpha \cap \mathbb{T}_\beta$, if

(1) D has coefficients 0 and 1 everywhere,

(2) D is topologically an embedded disk on Σ, with $2m$ vertices on its boundary,

(3) There is exactly one region with coefficient 1 around each vertex on the ∂D,

(4) D does not contain any points in A or B in its *interior*.

Once we have a nice Heegaard diagram $(\Sigma, \beta, \alpha, z)$, by [16], it is combinatorial to calculate the boundary map of the Heegaard Floer chain complex. We just make a list of all the generators and count all the empty embedded bigons and the empty embedded squares on the Heegaard surface connecting these generators by examining the diagram. Finally by using simple linear algebra with $\mathbb{Z}_2$ coefficients we can compute $\widehat{HF}(-Y)$. Here we emphasize that we can combinatorially determine all the generators which are mapped to the distinguished $Spin^c$ structure s_ξ, calculate $\widehat{HF}(-Y, s_\xi)$ and identify $c(\xi) \in \widehat{HF}(-Y, s_\xi)$. $\square$

2. The unique tight contact structure on $S^1 \times S^2$

Consider the contact 3-manifold (Y, ξ) described by the surgery diagram depicted in Figure 1. When we convert this diagram into a smooth diagram (cf. Figure 2) and blow down the -1-curve, we immediately see that the underlying 3-manifold Y is nothing but $S^1 \times S^2$. It is well-known that there exists a unique tight contact structure on $S^1 \times S^2$ up to isotopy [5].

Proposition 2. *The contact structure ξ is the unique tight contact structure on $S^1 \times S^2$.*

Proof. Below we show that the contact Ozsváth-Szabó invariant $c(\xi)$ is nontrivial. Therefore by a fundamental result in [13] ξ is tight. □

Remark 3. *In particular, the unique tight contact structure on $S^1 \times S^2$ has nontrivial contact Ozsváth-Szabó invariant. This was first proved in* [10].

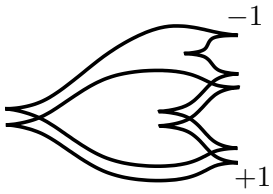

FIGURE 1. A contact surgery diagram

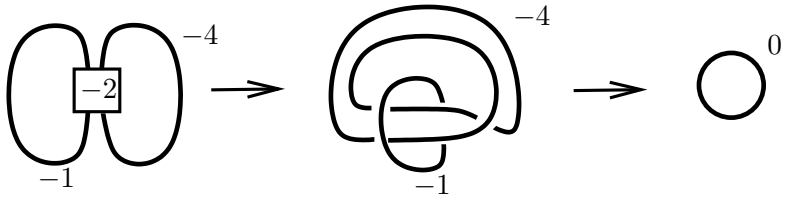

FIGURE 2. Underlying 3-manifold is $S^1 \times S^2$

First we would like to understand the homotopy class of ξ considered as an oriented plane field and determine the $Spin^c$ structure s_ξ induced by ξ. We calculate the first Chern class of ξ as follows: Let K_1 and K_2 denote the ± 1 surgery curves in Figure 1, respectively. Orient these Legendrian knots and let μ_1 and μ_2 denote the oriented meridians of K_1 and K_2, respectively. Then by [4] we have

$$PD(c_1(\xi)) = rot(K_1)[\mu_1] + rot(K_2)[\mu_2] = [\mu_1] + 2[\mu_2] = 0 \in H_1(S^1 \times S^2, \mathbb{Z})$$

where PD denotes the Poincare dual and $rot(K_i)$ denotes the rotation number of K_i. Moreover since $H_1(S^1 \times S^2; \mathbb{Z}) = \mathbb{Z}$ has no 2-torsion the $Spin^c$ structure s_ξ is determined by

$c_1(\xi)$. In other words s_ξ is the unique $Spin^c$ structure on $S^1 \times S^2$ whose first Chern class is trivial.

Our goal, however, is to calculate $\widehat{HF}(-Y, s_\xi)$, $\widehat{HF}(-Y)$ and in particular the contact Ozsváth-Szabó invariant $c(\xi) \in \widehat{HF}(-Y, s_\xi)$. By applying the techniques in [6] we can find an open book decomposition OB_ξ (see Figure 3) compatible with ξ: First we start with the open book decomposition OB_H induced by the positive Hopf link H in S^3, whose page is an annulus. Then we stabilize this open book decomposition once and embed the +1 surgery curve onto a page. Next we stabilize one more time and embed the -1 surgery curve onto a page. Applying the required surgeries we get the desired open book decomposition. Note that we get exactly the same open book considered by Plamenevskaya in [15]. By the lantern relation on the four punctured sphere we know that the monodromy of OB_ξ is a product of two right-handed Dehn twists and hence ξ is Stein fillable [8]. Therefore we know that the contact Ozsváth-Szabó invariant of ξ is nontrivial [13]. In the following we will verify this fact by the algorithm described in [15], but we will choose three different bases to illustrate that this choice is in fact crucial in calculations.

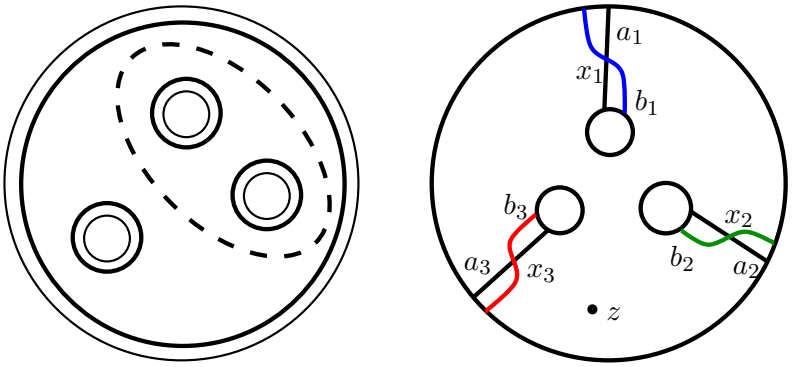

FIGURE 3. Left: Monodromy on a page of OB_ξ. Dehn twists about the solid curves are right-handed, while the Dehn twist about the dashed curve is left-handed. Right: A basis $\{a_1, a_2, a_3\}$ on the page $S_{1/2}$, the arcs $\{b_1, b_2, b_3\}$, the intersection points $\{x_1, x_2, x_3\}$, and the base point z.

2.1. **Basis I.** First we take the basis $\{a_1, a_2, a_3\}$ on page S which is shown on the right in Figure 3. This is the basis that was used in [15]. We observe that there are two "bad" regions, one non-disk the other a hexagon. We divide each of these regions into two square regions by a simple finger move ([15]) introducing a bigon in the process. The resulting curves are depicted in Figure 5. After this modification of the Heegaard diagram there are nine regions which do not contain z. These regions are denoted by $R_1, \ldots, R_9$ and labelled by their indices in Figure 5.

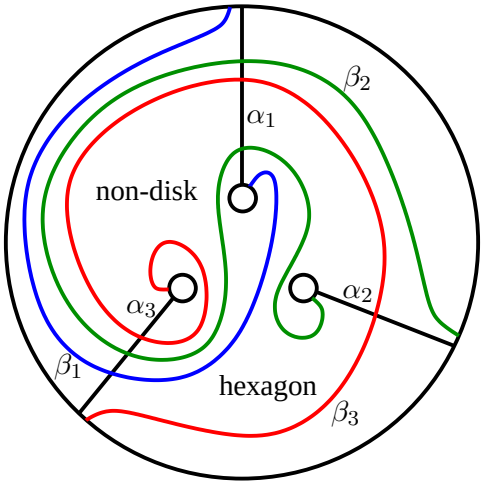

FIGURE 4. Bad regions are indicated on page S_0

Now by examining the intersections of α and β curves on Σ we see that the generators of the Heegaard Floer chain complex $\widehat{CF}(\Sigma, \beta, \alpha, z)$ are $X = (x_1, x_2, x_3), A = (x_1, z_1, v_3), B = (x_1, x_2, z_3), C_k = (y_k, x_2, z_2), D_{ij} = (v_i, w_j, z_3), E_{ij} = (v_i, w_j, x_3), F_i = (v_i, z_1, z_2), G_{kj} = (y_k, w_j, v_3)$, where $1 \leq i, j \leq 2$ and $1 \leq k \leq 3$. We calculated all the boundary maps induced by the empty embedded bigons and empty embedded squares:

$\partial X = 0$
$\partial A = B$ by $R_3 + R_4$
$\partial B = 0$
$\partial C_1 = 0$
$\partial C_2 = X + C_1$ by $R_4 + R_7 + R_8$ and R_9
$\partial C_3 = B$ by $R_4 + R_8$
$\partial D_{11} = B + G_{11} + D_{12}$ by R_1, R_5 and R_6
$\partial D_{12} = G_{12}$ by R_5
$\partial D_{21} = D_{22}$ by R_6
$\partial D_{22} = 0$
$\partial E_{11} = X + E_{12}$ by R_1 and R_6
$\partial E_{12} = 0$
$\partial E_{21} = E_{22}$ by R_6
$\partial E_{22} = 0$
$\partial F_1 = E_{12} + C_1$ by R_2 and $R_3 + R_4 + R_5$
$\partial F_2 = E_{22} + C_3 + A$ by R_2, R_3 and R_8
$\partial G_{11} = G_{12}$ by R_6
$\partial G_{12} = 0$

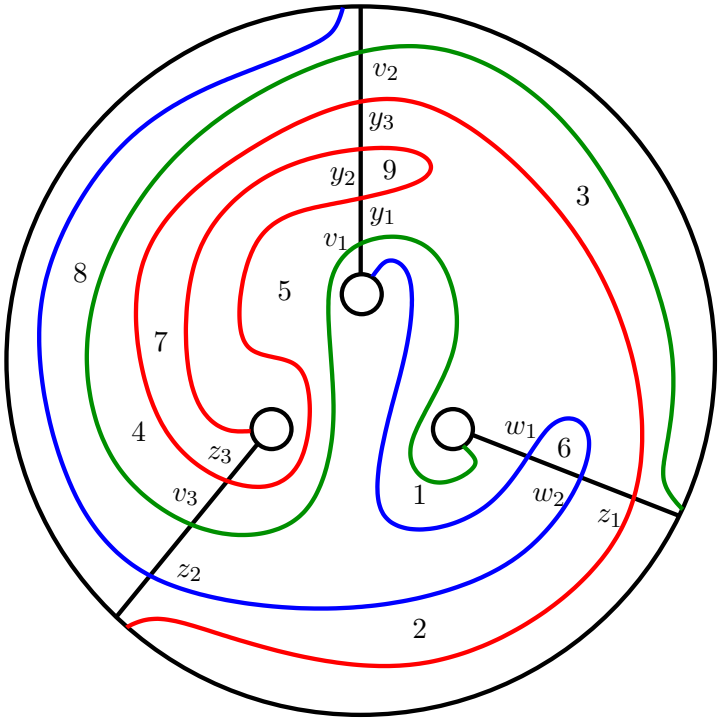

FIGURE 5. Curves, intersections and regions after the finger moves

$\partial G_{21} = E_{21} + G_{11} + G_{22}$ by $R_4 + R_7$, R_9 and R_6
$\partial G_{22} = E_{22} + G_{12}$ by $R_4 + R_7$ and R_9
$\partial G_{31} = D_{21} + G_{32}$ by R_4 and R_6
$\partial G_{32} = D_{22}$ by R_4

The generators split into two sets: In the first set we have the generators X, C_1, C_2, E_{11}, E_{12}, F_1 with the following boundary maps: $\partial X = 0$, $\partial C_1 = 0$, $\partial C_2 = X + C_1$, $\partial E_{12} = 0$, $\partial E_{11} = X + E_{12}$, $\partial F_1 = E_{12} + C_1$. Note that these generators all correspond to the $Spin^c$ structure s_ξ because we know ([9]) that the cycle X corresponds to s_ξ, and there are Whitney disks connecting X and C_2, C_2 and C_1, C_1 and F_1, F_1 and E_{12}, E_{12} and E_{11}. Similarly, there exist Whitney disks connecting the other 16 generators. Let V_1 be the vector space over $\mathbb{Z}_2$ generated by X, C_1, C_2, E_{11}, E_{12}, F_1 and let $\partial_1 : V_1 \to V_1$ denote the linear map induced by the boundary maps. Then it is easy to see that rank $\partial_1 = 2$ and dim $\ker \partial_1 = 4$. It follows that $\widehat{HF}(-S^1 \times S^2, s_\xi) = \mathbb{Z}_2 \oplus \mathbb{Z}_2$ which is generated by $[X] = c(\xi)$ and $[C_2 + E_{11} + F_1]$. Hence we conclude that $c(\xi) \neq 0$.

Remark 4. *In* [15], *Plamenevskaya argues that* $\partial E_{11} = X + E_{12}$ *(*$d\boldsymbol{x} = \boldsymbol{c} + \boldsymbol{y}$ *in her notation) is sufficient to show that* $[X] \neq 0$. *But in fact one has to show that* E_{12} *is not*

a boundary. For a complete argument one has take into account the boundary relations $\partial F_1 = E_{12} + C_1$ *and* $\partial C_2 = X + C_1$.

To see that the generators in the second set correspond to a different $Spin^c$ structure $s \neq s_\xi$, consider the loop Γ in the Heegaard surface Σ obtained by concatenating the following paths: part of α_1 from x_1 to v_2, part of β_2 from v_2 to x_2, part of α_2 from x_2 to z_1, part of β_3 from z_1 to x_3, part of α_3 from x_3 to z_2 and part of β_1 from z_2 to x_1. According to [12], the difference between the $Spin^c$ structures which correspond to $X = (x_1, x_2, x_3)$ and $F_2 = (v_2, z_1, z_2)$ is measured by the Poincaré dual of $p([\Gamma])$ in $H^2(S^1 \times S^2; \mathbb{Z})$, where

$$p : H_1(\Sigma; \mathbb{Z}) \to \frac{H_1(\Sigma; \mathbb{Z})}{< [\alpha_1], [\alpha_2], [\alpha_3], [\beta_1], [\beta_2], [\beta_3] >} \cong H_1(S^1 \times S^2; \mathbb{Z}) \cong \mathbb{Z}$$

is the quotient homomorphism. In Figure 6, the curve Γ is drawn on the Heegaard surface Σ together with γ_i's such that $[\gamma_i]$'s complete $[\alpha_i]$'s to a basis for the first homology of Σ.

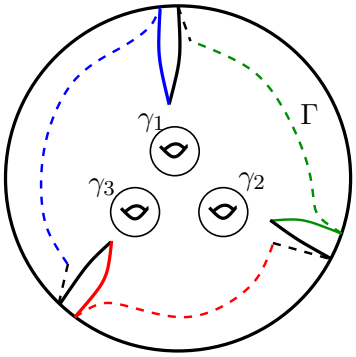

FIGURE 6. The curve Γ on the Heegaard surface $\Sigma = S_{1/2} \cup -S_0$. Here we depict Σ so that $S_{1/2}$ is on top which carries the solid curves and S_0 is at the bottom which carries the dashed curves.

On one hand $[\Gamma] = [\gamma_1] + [\gamma_2] + [\gamma_3] \in H_1(\Sigma; \mathbb{Z})$, where each of these curves is oriented "clockwise". On the other hand, the kernel of the quotient epimorphism p is generated by $[\gamma_1] + [\gamma_3]$, $[\gamma_2] + [\gamma_3]$ and $[\alpha_i]$'s (see Figure 7). Therefore $p([\Gamma])$ is $\pm 1 \in \mathbb{Z} \cong H_1(S^1 \times S^2; \mathbb{Z})$, in particular nonzero. This implies that the generators X and F_2 of the Heegaard Floer chain complex correspond to different $Spin^c$ structures, i.e. $s \neq s_\xi$.

Let V_2 be the vector space generated by the remaining generators and let $\partial_2 : V_2 \to V_2$ denote the boundary map. One can calculate by simple linear algebra that rank $\partial_2 = 8$ and dim $\ker \partial_2 = 8$. Hence we conclude that the homology for (V_2, ∂_2) is trivial, i.e., $\widehat{HF}(-S^1 \times S^2, s) = 0$. Since there are no other generators, the Heegaard Floer homology groups in the other $Spin^c$ structures are automatically zero. Consequently we get

$$\widehat{HF}(-S^1 \times S^2) = \widehat{HF}(-S^1 \times S^2, s_\xi) \oplus \widehat{HF}(-S^1 \times S^2, s) = \mathbb{Z}_2 \oplus \mathbb{Z}_2,$$

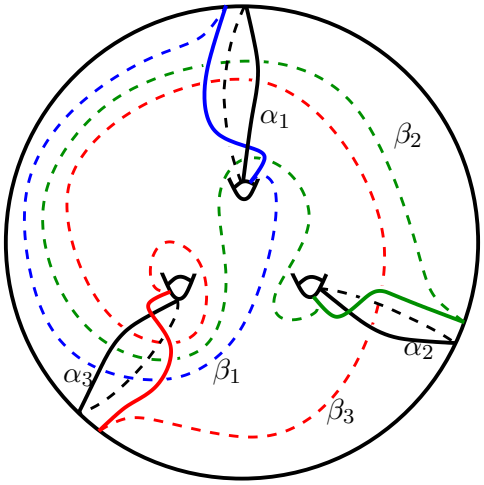

FIGURE 7. The α and β curves on $\Sigma = S_{1/2} \cup -S_0$ where we use the convention in Figure 6.

which was indeed proved in [12].

2.2. **Basis II.** In the following we choose a different basis on the page S of OB_ξ and repeat the calculations above. The point is that with this new choice of basis we will have fewer generators and fewer relations. We depict the α and β curves on page $S_{1/2}$ in Figure 8. Now by examining the intersections of α and β curves on Σ we see that there are exactly eight generators of the Heegaard Floer chain complex: $X = (x_1, x_2, x_3), A = (w_2, y_1, x_3), B = (x_1, y_2, x_3), C = (x_1, z_1, y_3), D = (w_2, y_3, z_2), E = (w_1, x_2, z_2), F = (w_1, y_2, z_2), G = (w_1, y_1, z_1)$.

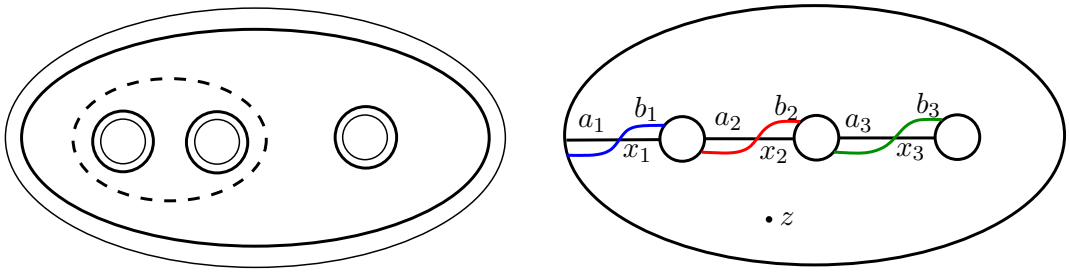

FIGURE 8. Left: Monodromy on a page of OB_ξ. Dehn twists about the solid curves are right-handed, while the Dehn twist about the dashed curve is left-handed. Right: A basis $\{\alpha_1, \alpha_2, \alpha_3\}$ on the page $S_{1/2}$, the arcs $\{b_1, b_2, b_3\}$, the intersection points $\{x_1, x_2, x_3\}$, and the base point z.

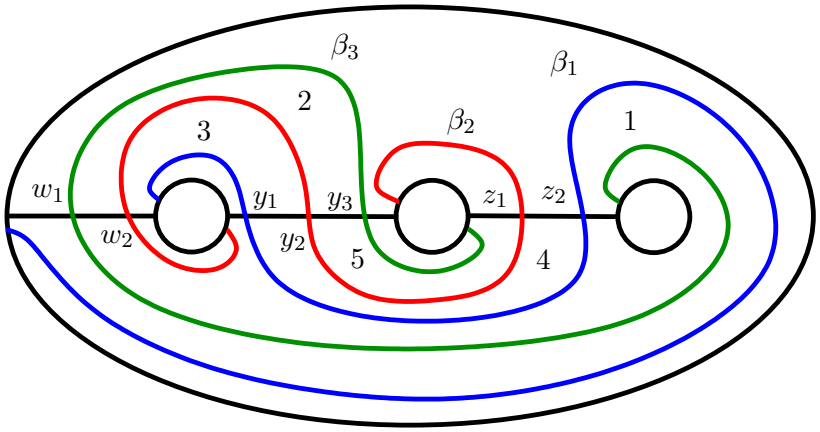

FIGURE 9. The α and β curves on page S_0

There are five regions which do not contain z. These are denoted by $R_1, \dots, R_5$ and labelled by their indices in Figure 9. Note that all of the regions are already squares. So we do not need to apply any finger moves. Below we list the boundary maps induced by these squares:

$\partial X = 0$
$\partial A = B$ by R_3
$\partial B = 0$
$\partial C = B$ by R_5
$\partial D = A + C$ by $R_3 + R_4$ and $R_4 + R_5$
$\partial E = X + X = 0$ by R_1 and $R_2 + R_3 + R_4 + R_5$
$\partial F = B + D + G + B = D + G$ by R_1, R_2, R_4 and $R_2 + R_3 + R_4 + R_5$
$\partial G = A + C$ by $R_2 + R_3$ and $R_2 + R_5$

The chain complex naturally splits with respect to the $Spin^c$ structures. The generators X and E correspond to the $Spin^c$ structure s_ξ which is uniquely determined by $c_1(s_\xi) = c_1(\xi) = 0$. The other generators correspond to a different $Spin^c$ structure $s \neq s_\xi$. To see this consider the loop Γ in the Heegaard surface Σ obtained by concatenating the following paths: part of α_1 from x_1 to w_1, part of β_3 from w_1 to y_3, part of α_2 from y_3 to x_2, part of β_2 from x_2 to z_1, part of α_3 from z_1 to z_2 and part of β_1 from z_2 to x_1. According to [12], the difference between the $Spin^c$ structures which correspond to $C = (x_1, y_3, z_1)$ and $E = (w_1, x_2, z_2)$ is measured by the Poincaré dual of $p([\Gamma])$ in $H^2(S^1 \times S^2; \mathbb{Z})$, where

$$p : H_1(\Sigma; \mathbb{Z}) \to \frac{H_1(\Sigma; \mathbb{Z})}{< [\alpha_1], [\alpha_2], [\alpha_3], [\beta_1], [\beta_2], [\beta_3] >} \cong H_1(S^1 \times S^2; \mathbb{Z}) \cong \mathbb{Z}$$

is the quotient homomorphism. In Figure 10, the curve Γ is drawn on the Heegaard surface Σ together with γ_i's such that $[\gamma_i]$'s complete $[\alpha_i]$'s to a basis for the first homology of Σ.

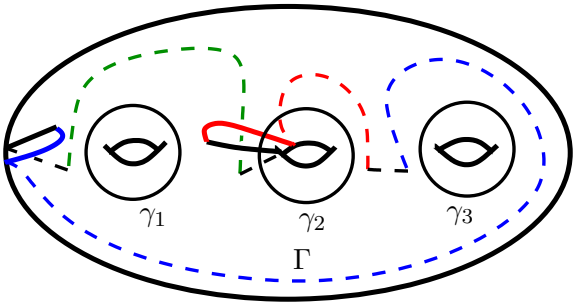

FIGURE 10. The curve Γ on the Heegaard surface $\Sigma = S_{1/2} \cup -S_0$ where we use the convention in Figure 6.

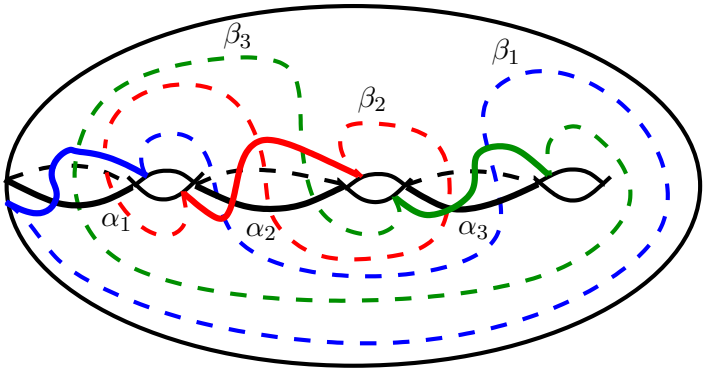

FIGURE 11. The α and β curves on $\Sigma = S_{1/2} \cup -S_0$ where we use the convention in Figure 6.

On one hand $[\Gamma] = [\gamma_1] + [\gamma_2] + [\gamma_3] \in H_1(\Sigma; \mathbb{Z})$, where each of these curves is oriented "clockwise". On the other hand, the kernel of the quotient epimorphism p is generated by $[\gamma_1] + [\gamma_3]$, $[\gamma_1] - [\gamma_2]$ and $[\alpha_i]$'s (see Figure 11). Therefore $p([\Gamma])$ is $\pm 1 \in \mathbb{Z} \cong H_1(S^1 \times S^2; \mathbb{Z})$, in particular nonzero. This implies that the generators C and E of the Heegaard Floer chain complex correspond to different $Spin^c$ structures, i.e. $s \neq s_\xi$. Moreover one can see that the homology induced by the generators $\{A, B, C, D, F, G\}$ is trivial. Therefore we conclude that $\widehat{HF}(-S^1 \times S^2) = \widehat{HF}(-S^1 \times S^2, s_\xi) = \mathbb{Z}_2 \oplus \mathbb{Z}_2$ which is generated by $[X]$ and $[E]$. This confirms again that the contact class $[X] = c(\xi) \neq 0$.

2.3. **Basis III.** Interestingly there is yet another basis which simplifies the calculations dramatically. The basis given in Figure 12 produces only two generators $X = (x_1, x_2, x_3)$, and $A = (y_1, x_2, y_3)$. Other than the one which contains the base point z, there are four regions $R_1, \ldots, R_4$ indicated in Figure 13 by their indices and these regions are already squares. Moreover $\partial A = X + X = 0$ by $R_1 + R_2$ and $R_3 + R_4$, and $\partial X = 0$, confirming

$\widehat{HF}(-S^1 \times S^2) = \widehat{HF}(-S^1 \times S^2, s_\xi) = \mathbb{Z}_2 \oplus \mathbb{Z}_2$, the nontriviality of the contact class $[X] = c(\xi)$ and consequently the tightness of ξ.

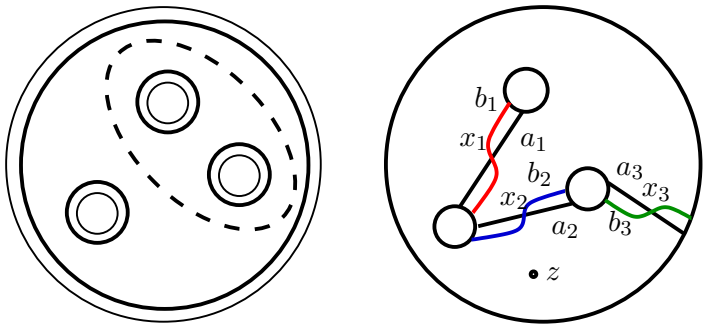

FIGURE 12. Left: Monodromy on a page of OB_ξ. Dehn twists about the solid curves are right-handed, while the Dehn twist about the dashed curve is left-handed. Right: A basis $\{a_1, a_2, a_3\}$ on the page $S_{1/2}$, the arcs $\{b_1, b_2, b_3\}$, the intersection points $\{x_1, x_2, x_3\}$, and the base point z.

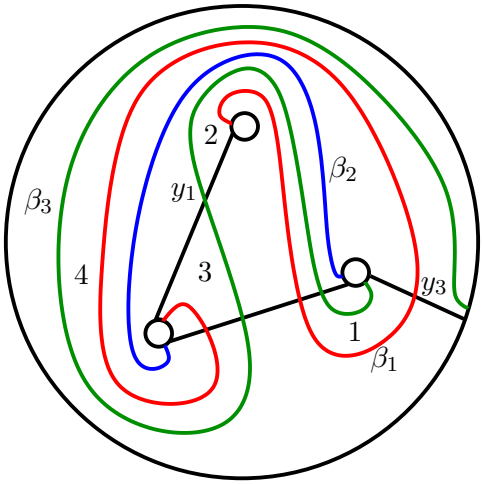

FIGURE 13. Curves, intersections and regions on page S_0

3. AN OVERTWISTED CONTACT STRUCTURE ON S^3

Consider the contact 3-manifold (Y, ξ) described by the surgery diagram depicted in Figure 14. When we convert this diagram into a smooth diagram (see Figure 15) and blow down the -1-curve, we immediately see that the underlying 3-manifold Y is homeomorphic to S^3. Note that there is a unique $Spin^c$ structure on S^3. From the contact surgery

diagram we obtain an open book decomposition OB_ξ on S^3 compatible with ξ shown on the left of Figure 16.

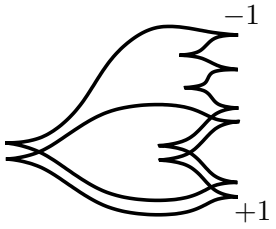

FIGURE 14. A contact surgery diagram

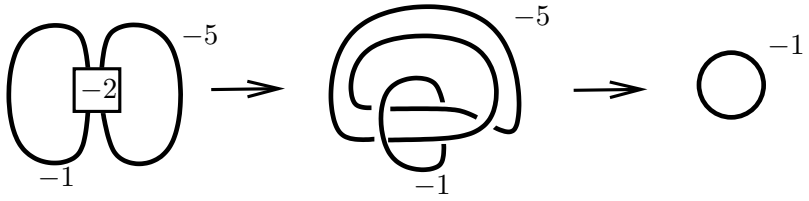

FIGURE 15. Underlying 3-manifold is S^3

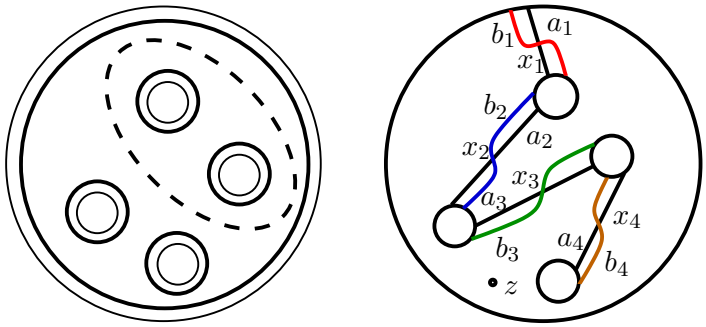

FIGURE 16. Left: Monodromy on a page of OB_ξ. Dehn twists about the solid curves are right-handed, while the Dehn twist about the dashed curve is left-handed. Right: A basis $\{a_1, a_2, a_3, a_4\}$ on the page $S_{1/2}$, the arcs $\{b_1, b_2, b_3, b_4\}$, the intersection points $\{x_1, x_2, x_3, x_4\}$, and the base point z.

Choosing a basis indicated on the right in Figure 16 gives the Heegaard diagram whose α and β curves are shown in Figure 17. It is possible to convert this Heegaard diagram into one without any bad region (except for the region including the base point z), by

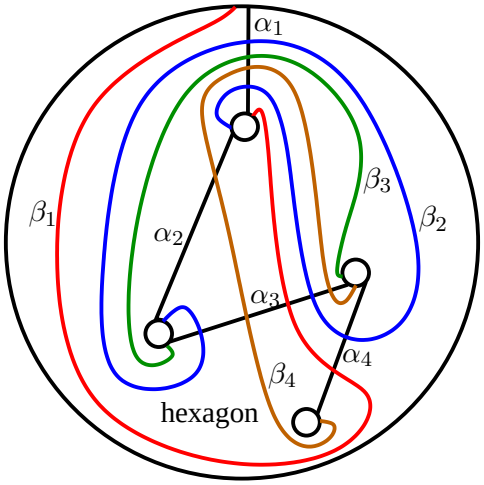

FIGURE 17. The bad region is indicated on page S_0

a simple finger move. The curves of this new Heegaard diagram are depicted in Figure 18. There are 13 regions which do not contain z. These regions are denoted by $R_1, \dots, R_{13}$ and labelled by their indices in Figure 18. Examining the intersections of α and β curves on the Heegaard surface Σ one can confirm that the Heegaard Floer chain complex $\widehat{CF}(\Sigma, \beta, \alpha, z)$ have 29 generators in total: $X = (x_1, x_2, x_3), A = (x_1, r, x_3, n)$, $B_{ij} = (v_i, t_j, x_3, x_4), C_{ij} = (v_i, z_j, u, x_4), D_{ij} = (v_i, r, u, w_j), E_i = (v_i, r, x_3, p)$, $F_k = (y_k, x_2, u, x_4)$, $G_k = (y_k, r, u, n), H_i = (q, t_i, x_3, n)$, $I_i = (q, x_2, u, w_i), J = (q, x_2, x_3, p)$, $K_i = (q, z_i, u, n)$, where $1 \leq i, j, \leq 2$ and $1 \leq k \leq 3$. One can also calculate all the boundary maps:

$\partial X = 0$
$\partial A = X$ by $R_9 + R_{11} + R_{12}$
$\partial B_{11} = B_{21}$ by R_4
$\partial B_{12} = X + B_{22}$ by $R_1 + R_2$ and R_4
$\partial B_{2j} = 0$
$\partial C_{11} = B_{12} + C_{21} + F_1$ by R_3, R_4 and R_1
$\partial C_{12} = B_{11} + C_{22}$ by $R_{11} + R_{13}$ and R_4
$\partial C_{21} = B_{22} + F_2$ by R_3 and $R_1 + R_5$
$\partial C_{22} = B_{21}$ by $R_{11} + R_{13}$
$\partial D_{11} = D_{21}$ by R_4
$\partial D_{12} = C_{12} + D_{22} + E_1$ by R_9, R_4 and R_{13}
$\partial D_{21} = 0$
$\partial D_{22} = C_{22} + E_2$ by R_9 and R_{13}
$\partial E_1 = B_{11} + E_2$ by $R_9 + R_{11}$ and R_4

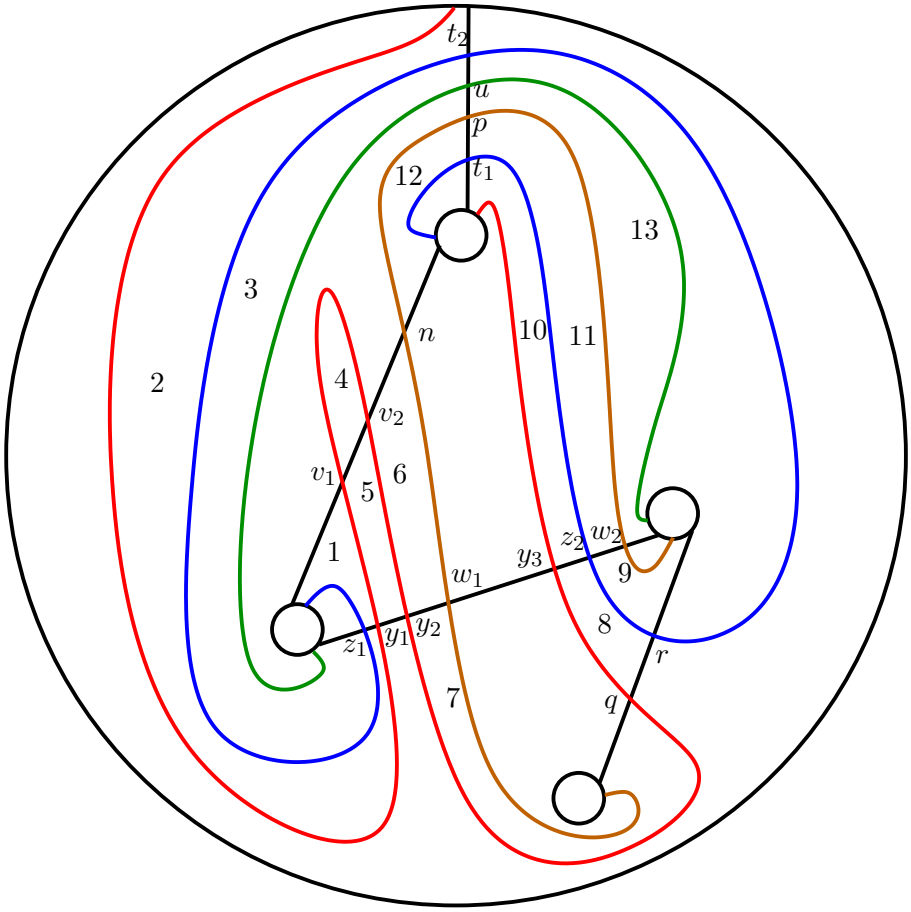

FIGURE 18. Curves, intersections and regions afer the finger move

$\partial E_2 = B_{21}$ by $R_9 + R_{11}$
$\partial F_1 = X + F_2$ by $R_2 + R_3$ and $R_4 + R_5$
$\partial F_2 = 0$
$\partial F_3 = X$ by $R_{10} + R_{11} + R_{13}$
$\partial G_1 = A + D_{11} + F_1 + G_2$ by $R_2 + R_3$, $R_5 + R_6$, $R_9 + R_{11} + R_{12}$ and $R_4 + R_5$
$\partial G_2 = D_{21} + F_2$ by R_6 and $R_9 + R_{11} + R_{12}$
$\partial G_3 = A + F_3$ by $R_{10} + R_{11} + R_{13}$ and $R_9 + R_{11} + R_{12}$
$\partial H_1 = A + B_{21} + J$ by $R_8 + R_{10}$, $R_6 + R_7$ and R_{12}
$\partial H_2 = B_{22}$ by $R_6 + R_7$
$\partial I_1 = F_2$ by R_7
$\partial I_2 = F_3 + J$ by $R_8 + R_9$ and R_{13}
$\partial J = X$ by $R_8 + R_9 + R_{10} + R_{11}$

$\partial K_1 = C_{21} + H_2 + I_1$ by $R_6 + R_7$, R_3 and $R_1 + R_5 + R_6$
$\partial K_2 = C_{22} + G_3 + H_1 + I_2$ by $R_6 + R_7$, R_8, $R_{11} + R_{13}$ and $R_{11} + R_{12}$

From $\partial A = X$ one immediately sees that $c(\xi) = [X] = 0 \in \widehat{HF}(-S^3, s_\xi)$ even with $\mathbb{Z}$ coefficients. By an important result in [13], ξ is not Stein fillable. In fact, since the unique tight contact structure on S^3 is Stein fillable by [5], ξ is overtwisted. On the other hand, it is seen that the image of the boundary map is 14 dimensional since it is generated by $\{X, B_{21}, B_{22}, D_{21}, F_2, A + F_3, A + J, B_{11} + C_{22}, B_{11} + E_2, B_{12} + C_{21} + F_1, A + D_{11} + F_1 + G_2, C_{12} + D_{22} + E_1, C_{21} + H_2 + I_1, C_{22} + G_3 + H_1 + I_2\}$. Therefore the kernel is $29 - 14 = 15$ dimensional. Hence we verified that $\widehat{HF}(-S^3, s_\xi) = \widehat{HF}(-S^3) = \mathbb{Z}_2$.

Remark 5. *Note that this contact structure has an open book decomposition which differs from the one in the previous section by an additional puncture and a right-handed Dehn twist around that puncture. It is interesting that these modifications, even though the Dehn twist is right-handed, convert a Stein fillable contact structure to an overtwisted one.*

Remark 6. *An alternative way to see the overtwistedness of the contact structure ξ given by the contact surgery diagram in Figure 14 is to use the d_3 invariant of ξ as a plane field and compare it with that of the unique tight contact structure on S^3. The former is $1/2$ whereas the latter is $-1/2$.*

Acknowledgement: We would like to thank András Stipsicz for comments on a draft of this paper. TE was partially supported by a GEBIP grant of the Turkish Academy of Sciences and a CAREER grant of the Scientific and Technological Research Council of Turkey. BO was partially supported by a research grant of the Scientific and Technological Research Council of Turkey.

REFERENCES

[1] S. Akbulut and B. Ozbagci, *Lefschetz fibrations on compact Stein surfaces*, Geom. Topol. **5** (2001), 319–334.
[2] M. F. Arikan, *On the support genus of a contact structure given by a surgery diagram*, preprint, arXiv:math.GT/0704.1670
[3] F. Ding and H. Geiges, *A Legendrian surgery presentation of contact 3-manifolds*, Math. Proc. Cambridge Philos. Soc. **136** (2004), 583–598.
[4] F. Ding, H. Geiges and A. Stipsicz, *Lutz twist and contact surgery,* Asian J. Math. 9 (2005), no. 1, 57–64.
[5] Y. Eliashberg, *Filling by holomorphic discs and its applications,* Geometry of low-dimensional manifolds, 2 (Durham, 1989), 45–67, London Math. Soc. Lecture Note Ser., 151, Cambridge Univ. Press, Cambridge, 1990.
[6] J. B. Etnyre, *Lectures on open book decompositions and contact structures,* Floer homology, gauge theory, and low-dimensional topology, 103–141, Clay Math. Proc., 5, Amer. Math. Soc., Providence, RI, 2006.

[7] J. B. Etnyre and B. Ozbagci, *Open books and plumbings*, Int. Math. Res. Notices vol. 2006, Article ID 72710, 2006.
[8] E. Giroux, *Contact geometry: from dimension three to higher dimensions*, Proceedings of the International Congress of Mathematicians (Beijing 2002), 405–414.
[9] K. Honda, W. Kazez and G. Matić, *On the contact class in Heegaard Floer homology*, preprint, arXiv:math.GT/0609734
[10] P. Lisca and A. I. Stipsicz, *Seifert fibered contact three-manifolds via surgery*, Algebr. Geom. Topol. 4 (2004), 199–217 (electronic).
[11] B. Ozbagci and A. I. Stipsicz, *Surgery on contact 3–manifolds and Stein surfaces*, Bolyai Soc. Math. Stud., Vol. **13**, Springer, 2004.
[12] P. Ozsváth and Z. Szabó, *Holomorphic disks and topological invariants for closed three-manifolds*, Ann. of Math. (2) 159 (2004), no. 3, 1027–1158.
[13] P. Ozsváth and Z. Szabó, *Heegaard Floer homology and contact structures*, Duke Math. J. 129 (2005), no. 1, 39–61.
[14] O. Plamenevskaya, *Contact structures with distinct Heegaard Floer invariants*, Math. Res. Lett. 11 (2004), no. 4, 547–561.
[15] O. Plamenevskaya, *A combinatorial description of the Heegaard Floer contact invariant*, to appear in Algebr. Geom. Topol., arXiv:math.GT/0612322
[16] S. Sarkar and J. Wang, *An algorithm for computing some Heegaard Floer homologies*, preprint, arXiv:math.GT/0607777
[17] S. Schönenberger, *Planar open books and symplectic fillings*, PhD thesis, University of Pennsylvania, 2005.
[18] A. I. Stipsicz, *Surgery diagrams and open book decompositions of contact 3-manifolds*, Acta Math. Hungar. 108 (2005), no. 1-2, 71–86.

DEPARTMENT OF MATHEMATICS, KOÇ UNIVERSITY, ISTANBUL, TURKEY
E-mail address: tetgu@ku.edu.tr
E-mail address: bozbagci@ku.edu.tr